Batchelor, A.R. and Jones, D.A. and Plint, S. and Kingman, S.W. (2015) Deriving the ideal ore texture for microwave treatment of metalliferous ores. Minerals Engineering, 84 . pp. 116-129. ISSN 0892-6875

Minerals Engineering 84 (2015) 116-129

Deriving the ideal ore texture for microwave treatment of metalliferous ores

A.R. Batchelor *, D.A. Jones, S. Plint, S.W. Kingman

Faculty of Engineering, The University of Nottingham, University Park, Nottingham, NG7 2RD, United Kingdom

* Corresponding author. Tel.: +44 (0)115 951 4080; fax: +44 (0)115 951 4115. E-mail address: andrew.batchelor@nottingham.ac.uk (A.R. Batchelor)

Keywords

Microwave; Ore; Mineralogy; Comminution.

Highlights

- The influence of mineralogy on microwave-induced fracture in ores is investigated
- Microwave-heating phase and matrix thermo-mechanical properties are both important
- Hard microwave-heating phases constrained by a hard matrix gave the best results
- ~2-20%wt heating phase abundance with grain size d50 >500µm gave the best results
- Ore textural consistency is required for high average strength reductions

Abstract

High power density microwave treatments on metalliferous ores have historically been shown to reduce ore competency prior to beneficiation at economically feasible energy inputs. However, the relationship between mineralogical textural features and the extent of the microwave-induced fracturing had previously been limited to qualitative descriptions or simplistic two-phase numerical models, which could not account for the complex mineral assemblages in real ores. In this paper, mineralogy, grain size, dissemination, textural consistency and mineral associations were determined for 13 commercially exploited nickel, copper and lead-zinc ores using a Mineral Liberation Analyser (MLA). The ores were subjected to high power density microwave treatments at up to 25kW in a single mode cavity with microwave energy inputs of approximately 0.5-10kWh/t, and the subsequent reductions in ore competency were measured by the Point Load Test. The ores that demonstrated the greatest reductions in strength typically contained between approximately 2%wt to 20%wt of highly microwave-absorbing minerals, with a native grain size d50 greater than approximately 500µm, constrained by hard matrix minerals such as quartz and feldspar. Texturally consistent ores with a high proportion of amenable textures also demonstrated the highest average reductions in strength. These findings support the qualitative descriptions and numerical modelling results available in the literature and provide a baseline for selecting likely candidate ores for microwave treatments in the future.

http://dx.doi.org/10.1016/j.mineng.2015.10.007

1 Introduction

On the basis of current and anticipated future reserves and rates of consumption, demand is predicted to outstrip supply for many mineral commodities within the next century (Kesler, 2007; Mudd, 2010). As higher grade ore bodies are exhausted, the average grades of the remaining deposits will diminish requiring even greater volumes of ore to be milled to meet the growing demand (Crowson, 2012; Mudd et al., 2013; Northey et al., 2014; Prior et al., 2012). It is also well established that comminution is the most energy intensive stage of mineral processing and that the process is inherently inefficient (Batterham, 2011; BCS, 2007; Curry et al., 2014; Nadolski et al., 2014; Tromans, 2008). Furthermore, new ore bodies are often more complex, occurring in harder rock with finer grain sizes, which further increases the energy required to liberate the valuable minerals for downstream separation processes (Cooke et al., 2006; Norgate and Jahanshahi, 2011; Sillitoe, 2010).

This growing demand for raw materials combined with a higher embodied energy in their production, rising costs, environmental and socio-political pressures will place a strain on sustainable mining in the future. In an effort to address these challenges, the aims of energy efficiency strategies in comminution include (Daniel and Lewis-Gray, 2011; Drinkwater et al., 2012; Pokrajcic et al., 2009; Powell and Bye, 2009):

- Reducing ore competency (i.e. AG/SAG mill impact breakage and abrasion parameters, and Ball Mill Work Index),
- Improving liberation to effect separation at a coarser size,
- More efficient crushing and grinding equipment and circuit design,
- Pre-concentration or barren waste rejection, and
- Indirectly reduce the burden on energy and materials from the production and consumption of consumables, such as water, grinding media and wear liners.

Microwave treatment has been proposed as a technique to reduce ore competency prior to beneficiation and as a means of enhancing liberation through the generation of thermally-induced cracks along mineral grain boundaries (Haque, 1999; Jones et al., 2002; Kingman and Rowson, 1998). The efficacy of this mechanism and the amenability of ores to microwave-induced fracture depend on the dielectric, thermal and mechanical properties of the minerals involved and their assemblage within ores.

1.1 Microwave treatment of ores

Thermally-assisted liberation has been widely cited as a means of reducing the competency of ores. Differential thermal expansion of the constituent minerals within the ore occurs during heating and cooling cycles, which results in the generation of significant stresses within the ore particles leading to fracture (Fitzgibbon and Veasey, 1990; Veasey and Wills, 1991). Using microwaves as the heating source offers particular benefits in that it provides rapid volumetric heating throughout the ore of only selected mineral phases, thereby eliminating the need to rely on conduction to transfer heat, significantly increasing heating rates and reducing energy requirements for fracture.

Work on microwave-assisted fracture and liberation has been carried out since the US Bureau of Mines worked extensively in this area during the 1980s, measuring the dielectric properties and low power (1-2.6kW, such as that used in domestic kitchen microwaves) heating rates of many common ore-forming minerals (Chen et al., 1984; Chunpeng et al., 1990; Church et al., 1988; Harrison, 1997; Kobusheshe, 2010; McGill and Walkiewicz, 1987; Nelson et al., 1989; Standish and Worner, 1991; Walkiewicz et al., 1988; Yixin and Chunpeng, 1996). These studies demonstrated that most aluminosilicates, micas, carbonates and sulphates (rock-forming minerals) showed little heating (i.e. microwave-transparent, ε''<0.3, <0.3°C/s), whereas most sulphides and metal oxides (economically important and associated gangue minerals) readily heated when exposed to microwave energy (i.e. microwave-absorbent, ε''>0.3, >0.3°C/s).

Studies by McGill et al. (1988) and Kingman et al. (2000b) also demonstrated that higher microwave power levels resulted in faster heating rates of many microwave-absorbing minerals. Subsequent experimental studies by Kingman et al. (2000a), Kingman et al. (2004a), Kingman et al. (2004b) and Sahyoun et al. (2005) revealed that high power density treatments (typically >3kW in single mode cavities) allowed for a similar degree of microwave-assisted breakage at significantly lower energy inputs than treatments at low power density (typically <3kW in multimode cavities) due to the significantly higher heating rates attained.

The energy required from low power density microwave treatments (typically >>10kWh/t) outweighed any potential energy saving during comminution processes and the high residence times (typically >>1s) would prohibit processing at a scale of several thousand tonnes per hour demanded by the mining industry. These studies, therefore, demonstrated microwave treatments at economically feasible energy inputs (<5kWh/t) and residence times (<1s) that could potentially achieve industrially relevant throughputs.

http://dx.doi.org/10.1016/j.mineng.2015.10.007

1.2 The role of mineralogy in microwave treatment of ores

Kingman et al. (2000b) also looked at the effects different mineralogies had on the change in Ball Mill Work Index after low power density microwave treatment for an ilmenite ore, refractory gold ore and two copper ores. The authors found that the most responsive ores were those with a consistent texture with relatively coarse grained microwave-absorbent minerals constrained by a microwave-transparent matrix. In contrast, the poorly performing ores had a relatively fine microwave-absorbent phase grain size that was sparsely disseminated.

Batchelor (2013) reviewed published literature from the previous 20 years detailing experiments using high and low power density microwave treatments on metalliferous ores investigating reduced ore competency. The vast majority of the papers reported findings on single ore samples, most with limited qualitative descriptions of mineralogy, grain size and/or mineral associations. By collating the information available and accounting for the different treatment regimens the author determined that, in addition to the findings by Kingman et al. (2000b), the ores that performed best typically had a matrix comprised of hard minerals (such as quartz, feldspar, pyroxene and olivine) rather than softer minerals (such as clays, carbonates or micas) coupled with a highly microwave-absorbent phase (such as magnetite).

For complex ores it is difficult to ascertain which combinations of minerals gives rise to the most significant strength reductions through experimentation. Numerical modelling studies have illustrated the mechanism of selective heating and thermally-induced fracture by considering binary systems of two differing mineral phases with varying thermo-mechanical properties, modal abundance, grain size, grain shape and dissemination (Ali and Bradshaw, 2009, 2010, 2011; Jones et al., 2005, 2007; Salsman et al., 1996; Wang et al., 2008; Wang and Djordjevic, 2014; Whittles et al., 2003). These studies have elucidated that the two important criteria for microwave-induced fracture are microwave power density and microwave energy input. Higher power density simulations always yielded a higher degree of particle damage for a given microwave energy input. However, for a given microwave power density there existed a minimum microwave energy input to provide sufficient thermal expansion and thermal gradients to initiate and propagate significant intergranular and transgranular fractures. In summary, the higher the heating rate, the less time there is for conduction to occur between adjacent grains, the greater the “thermal shock” (or thermally induced stresses) and the lower the microwave energy requirement. The authors suggested that a power density within the microwave-absorbent grains of greater than approximately $1x10^{10}$ W/m³ provided the most efficient fracture generation.

The aforementioned numerical modelling studies further demonstrated the following observations. Minerals that heat better in a microwave field and that have a high thermal expansion coefficient tended to generate fractures more readily due to higher heating rates and volumetric expansion. Finer microwave-absorbent grains, typically less than approximately 100µm in size, have been shown to yield less fracture than coarser grains, typically greater than approximately 500µm, attributed to a rapid loss of heat through conduction to the matrix due to the greatly increased surface area to volume compared to coarser grains. The loss of heat reduces the thermal shock and therefore requires a higher power density and/or energy input to raise the stress enough to cause significant fracture. A higher modal abundance and even dissemination of microwave-absorbent grains promoted fracture networking across the fragment, which reduced overall fragment competency; however, clustering of mineral grains helped to promote more intense localised fracturing. Finally, stronger/stiffer, or ‘harder”, minerals (such as quartz, feldspar and pyrite, as opposed to micas and chalcopyrite for example) could not deform elastically to absorb the thermal expansion and therefore generated larger stresses leading to an increased prevalence of fracture.

In summary, it has been elucidated from the literature that coarser grains of hard and highly microwave-absorbent minerals constrained by a hard microwave-transparent matrix provide the most favourable texture for initiation and propagation of fractures. From the numerical and experimental studies reviewed it is clear that it is important to consider the following ore characteristics:

- Microwave-absorbent (heating) phases
    - Abundance
    - Grain size
    - Dissemination
    - Textural consistency
    - Thermal expansion coefficient
    - Mechanical properties
- Microwave-transparent (non-heating) phases
    - Mechanical properties
    - Association with microwave-absorbent phases

http://dx.doi.org/10.1016/j.mineng.2015.10.007

This investigation evaluates the response of 13 distinct ores to high power density microwave treatments at different energy inputs. Mineralogical features such as modal abundance, grain size and mineral associations were measured with the aim of quantitatively and qualitatively relating mineralogical and textural features to the extent of reduction in ore competency in order to determine the ideal ore texture for microwave treatment.

2 Materials and methods

2.1 Ore samples

The ore samples used throughout this investigation were sourced from a variety of host mines and mining companies around the world including Australia, Chile, USA, South Africa and Europe. Some of the samples were from a different location within the same mine to investigate different mine lithologies. The samples were selected to represent a range of commodity types and mineralogical features likely to be encountered by microwave processing in industry.

The ores included three nickel ores, six copper ores and four lead-zinc ores. The ores were supplied in a variety of fragment sizes and forms, including core, SAG mill feed, sized ore and large lump ore. As such, some of the samples required screening or other preparation to achieve particulate form; therefore, not all ores were tested as natural fragments in the same size class.

Ni-Ore 1 was provided as -22.4+19.0mm fragments, Ni-Ore 3 as -37.5+26.5mm fragments, and Ni-Ore 2 as quartered 50mm core, which was further sawn into 15-30mm pieces. Cu-Ore 1-6 and Pb/Zn-Ore 3-4 were all supplied as SAG mill feed and screened into -37.5+19.0mm fragments. Pb/Zn-Ore 1-2 were supplied as 100-200mm lumps, which were sawn into approximately 15-30mm cuboids.

2.2 Mineralogical characterisation

Mineralogical and textural information for each of the ores was characterised by using a Mineral Liberation Analyser (MLA) to investigate cross-sections of approximately 15 to 30 lump fragments up to 30mm in diameter. Similar to liberation analysis on milled material, the MLA provided modal mineralogy, mineral grain size and mineral association information that resulted in quantitative textural data of the natural mineral assemblage in lump fragments.

15 to 30 fragments of each ore were selected to obtain a broad sense of their characteristics. Whilst it was appreciated that this number of fragments may be considered as insufficient to constitute a representative sample, the authors experience has shown that this number of fragments is sufficient to provide an appropriate representation for ores that have a fairly homogeneous texture. However, for the ores that exhibited a wide variety of textures (such as Ni-Ore 1, Cu-Ore 1 and Cu-Ore 2), the fragment count was increased to between 80-120 fragments.

In addition to providing individual mineral phase analysis, minerals were combined into certain groups to identify textural relationships. Minerals groups commonly included total copper or nickel sulphides (as opposed to individual copper or nickel minerals) as the valuable phase of interest, iron and other sulphides (typically the dominant microwave-heating phase), other microwave-heating phases (such as iron oxides and hydrated clays) and total microwave-heating phases.

Minerals were also classified according to their ‘hardness’. Hardness can be defined in many ways, such as elastic modulii, tensile and compressive strengths, or fracture toughness with respect to initiation and propagation of grain boundary or transgranular fracture. For ease of classification the Mohs hardness scale was used since it is a relative measure of resistance to mechanical damage with minerals falling in categories 1-3 classed as ‘soft’ minerals, 4-5 as ‘medium’ minerals and 6-10 as ‘hard’ minerals. In this way, the association of microwave-heating phases with hard or soft non-heating phases may be linked to any changes in comminution behaviour.

2.3 Microwave treatment apparatus

Microwaves were provided by a 3-15kW variable power Sairem generator and a 3-30kW variable power IBF Electronic generator, both operating at 2.45GHz. The generator was connected by rectangular WR430 waveguide to an E-H automatic impedance matching device (or tuner) with a circulator in the transmission line to dissipate reflected power in a water load. The tuner was then connected to a TE_{10n} single mode cavity and finally a short circuit tuner. A schematic illustration of the microwave system is given in Figure 1.

http://dx.doi.org/10.1016/j.mineng.2015.10.007

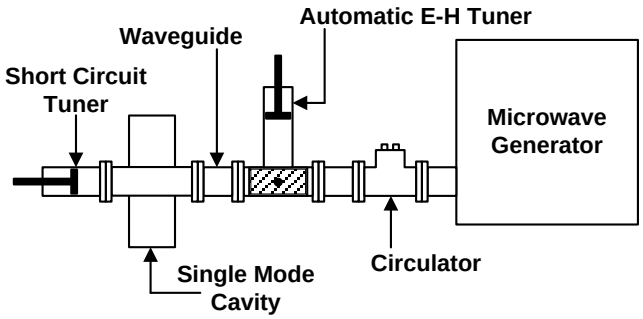

Figure 1: Microwave treatment apparatus

The TE_{10n} cavity was comprised of a hollow cylindrical tube section with an internal diameter of 82mm intersecting the broadside of the waveguide. Up to 1.5kg of ore load was placed in a one litre borosilicate glass tube supported by an alumina block that could then pass through the cavity. The test sample was preceded by sacrificial ore to absorb microwave energy during the microwave power ramp up cycle in order to ensure that the test sample received microwave energy at steady state and to ensure the system was well matched. Residence time within the cavity was then controlled using a pneumatic piston with an adjustable stroke, shown in Figure 2. The borosilicate glass tube, alumina supporting block and plastic piston rod were constructed from microwave-transparent materials (ε"<0.01) (Meredith, 1998) so that only the ore load would absorb microwave energy.

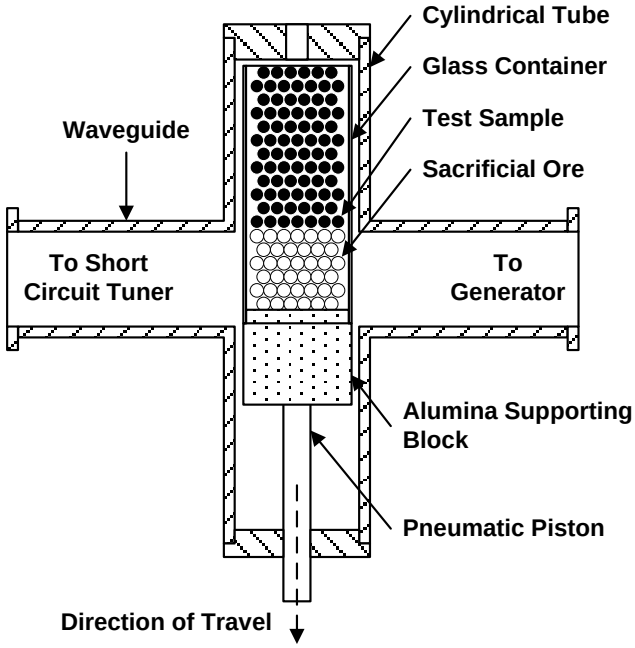

Figure 2: Single mode cavity apparatus

2.4 Microwave treatments

Microwave treatments were conducted with incident microwave powers of 15-25kW. The reflected power was subtracted from the incident power to determine the power absorbed by the load. Individual treatment masses were recorded and the stroke speed was set to achieve microwave energy inputs between approximately 1-15kWh/t. The resulting exposure times were the residence time of the ore within the waveguide section, which is in the region of the maximum electric field strength. For the shortest exposure times, the stroke speed was near free fall. The averaged microwave treatment conditions and number of fragments used in subsequent comminution testing are given in Table 1.

http://dx.doi.org/10.1016/j.mineng.2015.10.007

Table 1: Microwave treatment conditions

Parameter	Units	Ni-Ores			Pb/Zn-Ores				Cu-Ores					
		1	2	3	1	2	3	4	1	2	3	4	5	6
Untreated														
Fragments	#	370	95	57	70	59	92	233	123	105	218	184	85	100
Treated 1														
Fragments	#	150	96	76	62	53	106	174	123	105	204	176	85	100
Incident Power	kW	15.0	20.0	15.0	23.0	20.0	14.9	13.8	23.0	20.0	15.0	15.0	20.0	20.0
Absorbed Power	kW	14.0	18.5	14.0	20.0	13.0	13.9	12.3	20.0	18.0	13.0	13.0	13.0	16.0
Exposure Time	s	0.20	0.05	0.10	0.05	0.05	0.10	0.10	0.05	0.05	0.09	0.07	0.05	0.09
Dose	kWh/t	4.3	1.0	2.0	0.9	0.5	2.2	1.1	1.2	1.1	1.8	1.2	0.8	1.8
Treated 2														
Fragments	#	326	97	76	68	58	91	164	-	-	187	-	85	-
Incident Power	kW	15.0	23.0	15.0	23.0	22.0	14.8	15.0	-	-	15.0	-	20.0	-
Absorbed Power	kW	14.0	20.0	14.0	21.0	15.0	13.9	13.4	-	-	13.4	-	10.0	-
Exposure Time	s	0.79	0.22	0.29	0.22	0.22	0.50	0.22	-	-	0.17	-	0.22	-
Dose	kWh/t	14.2	4.8	7.2	4.0	2.4	11.5	2.4	-	-	3.5	-	2.8	-
Treated 3														
Fragments	#	-	-	-	67	58	-	-	-	-	-	-	-	-
Incident Power	kW	-	-	-	24.0	21.0	-	-	-	-	-	-	-	-
Absorbed Power	kW	-	-	-	20.0	14.0	-	-	-	-	-	-	-	-
Exposure Time	s	-	-	-	0.54	0.54	-	-	-	-	-	-	-	-
Dose	kWh/t	-	-	-	9.4	4.1	-	-	-	-	-	-	-	-

2.5 Comminution testing

Given the large number of samples under test and the limited mass available in many of the samples, a rapid strength assessment technique was required that did not require a large amount of material for comparative analysis of untreated and microwave-treated material. The Point Load Test fits these criteria as well as being a test that exploits any weakness in the ore by measuring the minimum force required for a first breakage event.

The Point Load Test was originally developed to test the strength of drill core and report a Point Load Index, I_S. The index is calculated by measuring the core diameter and the load required for breakage when applied to the core diametrically through two platens, given in Eq. (1) (Broch and Franklin, 1972; Franklin, 1985). The method was later adapted by Brook (1985) to test irregular lump fragments by measuring the equivalent core diameter based on fragment cross-sectional area and applying a correction factor to scale to a reference core size of 50mm, given in Eqs. (2) and (3) respectively. By combining Eqs. (1), (2) and (3) the corrected Point Load Index, $I_{S(50)}$, may be determined, given in Eq. (4).

$$I_S = P/D^2 \quad (1)$$

$$D_e = (4WH/\pi)^{0.5} \quad (2)$$

$$F = (D/50)^{0.45} \quad (3)$$

$$I_{S(50)} = (D/50)^{0.45}(P/D^2) \quad (4)$$

Where $I_{S(50)}$ is the corrected Point Load Index (MPa), I_S is the uncorrected Point Load Index (MPa), P is the force applied at failure (kN), F is the core size correction fraction, D_e is the equivalent core diameter for irregular fragments (mm), D is the core diameter or equivalent core diameter (mm), W is the fragment width (mm) and H is the fragment depth (mm).

http://dx.doi.org/10.1016/j.mineng.2015.10.007

The distribution of Point Load Indices of the fragment populations may be compared by ordering the fragments from softest to hardest on a cumulative mass basis, illustrated in Figure 9 to Figure 21. The mass-weighted average Point Load Indices may also be calculated from the populations to determine the average reduction in Point Load Index, or remaining strength, for the untreated and microwave-treated materials.

Statistical analyses of the Point Load tests have demonstrated that populations of approximately 100 fragments are typically required to achieve at least a 90% confidence level from a t-test for less than a 10% reduction in the average Point Load Index on microwave-treated material. Where less than approximately 100 fragments have been used, the average reduction may not be statistically significant, but reviewing the Point Load Index distributions and visually inspecting the fragments demonstrated the presence of fractures and weakened fragments, illustrated in Figure 3 for Ni-Ore 2.

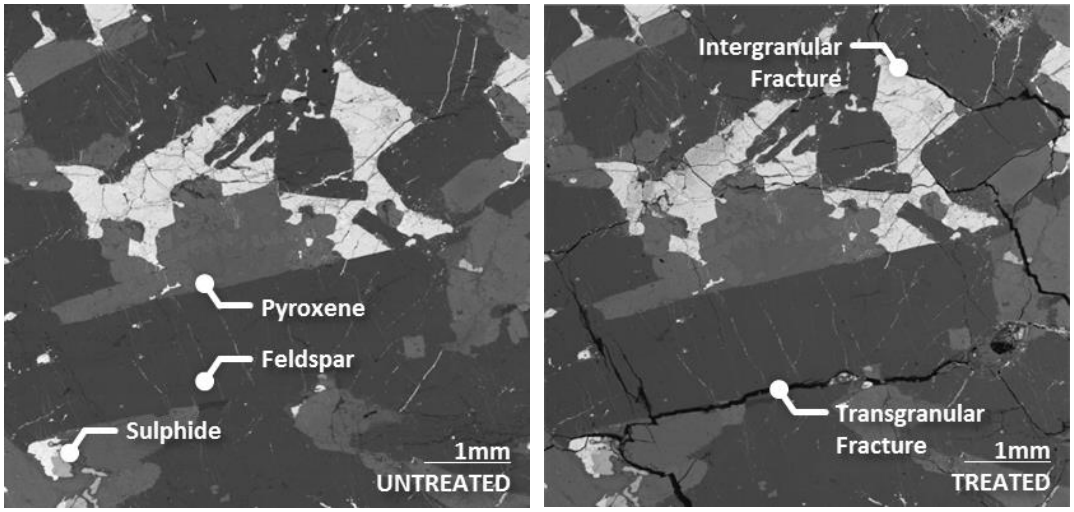

Figure 3: Ni-Ore 2 microwave-induced fracture

3 Results

3.1 Mineralogical characterisation

The mineralogical characterisation of the ores revealed the major microwave-heating minerals were nickel sulphides, copper sulphides, iron sulphides, galena, magnetite and hydrated clays such as hydrotalcite and smectite (classified as montmorillonite). Other poorly microwave-heating phases included iron oxides such as haematite, other Fe/Ti oxides and sphalerite.

The non-microwave-heating gangue minerals comprising the matrix of the ores typically included ‘hard’ quartz, feldspars, amphiboles and pyroxenes, with ‘soft’ micas (e.g. biotite, muscovite and illite), other phyllosilicates (e.g. talc, kaolinite, pyrophyllite and chlorite-group minerals), carbonates (e.g. calcite, magnesite and dolomite) and serpentine-group minerals.

http://dx.doi.org/10.1016/j.mineng.2015.10.007

3.1.1 Nickel ores

Example MLA texture images for the three nickel ores under investigation are given in Figure 4 with grouped mineral classifications of interest. The corresponding average modal mineralogy is given in Table 2.

Ni-Ore 1 was a blended concentrator feedstock derived from several mining areas of a komatiite deposit. As such, the blended ore had a wide variety of textures from massive sulphide to sulphide-barren with both discrete and veined sulphide mineralisation. The microwave-heating minerals were somewhat associated with hard quartz, feldspars and amphiboles, but predominantly with soft micas and carbonates.

Ni-Ore 2 was exploration drill core from a gabbronorite deposit. The ore had a consistent texture with the matrix dominated by two hard minerals, namely pyroxene and feldspars. Sulphide mineralisation was relatively coarse with copper and nickel sulphides highly associated with iron sulphides. Sulphide mineralisation tended to occur along the grain boundaries of the two matrix minerals.

Ni-Ore 3 was a serpentinized dunite ore with a consistent texture comprised of thin veins of predominantly magnetite running extensively throughout a soft serpentine matrix. Nickel sulphide grains were discretely disseminated consistently through the fragments measured.

Table 2: Modal mineralogy for the nickel ores

Heating Class	Mineral Name	Modal Abundance (%wt)		
		Ni-Ore 1	Ni-Ore 2	Ni-Ore 3
Good-MW Heater	Pentlandite	6.3	1.5	0.9
	Chalcopyrite	0.7	1.0	<0.1
	Iron Sulphides [a]	12.5	7.8	0.0
	Magnetite	1.9	0.8	10.5
	Hydrotalcite [b]	-	-	3.4
Poor-MW Heater	Iron Oxides [c]	0.7	0.9	0.2
Non-MW Heating Gangue	Amphibole	25.1	-	-
	Pyroxene	-	41.4	-
	Serpentine	-	-	81.2
	Mica-Phyllosilicate [d]	25.2	2.1	-
	Feldspar	14.0	43.8	-
	Carbonates [e]	10.8	-	0.2
	Quartz	2.5	0.1	-
	Other	0.3	0.7	3.7

[a] Predominantly pyrrhotite with minor pyrite; [b] includes woodallite and iowaite; [c] Fe/Ti/Cr oxides including chromite and ilmenite; [d] predominantly talc in Ni-Ore 1 with some chlorite and biotite, solely biotite in Ni-Ore 2; [e] roughly equal proportions of magnesite, calcite and dolomite.

http://dx.doi.org/10.1016/j.mineng.2015.10.007

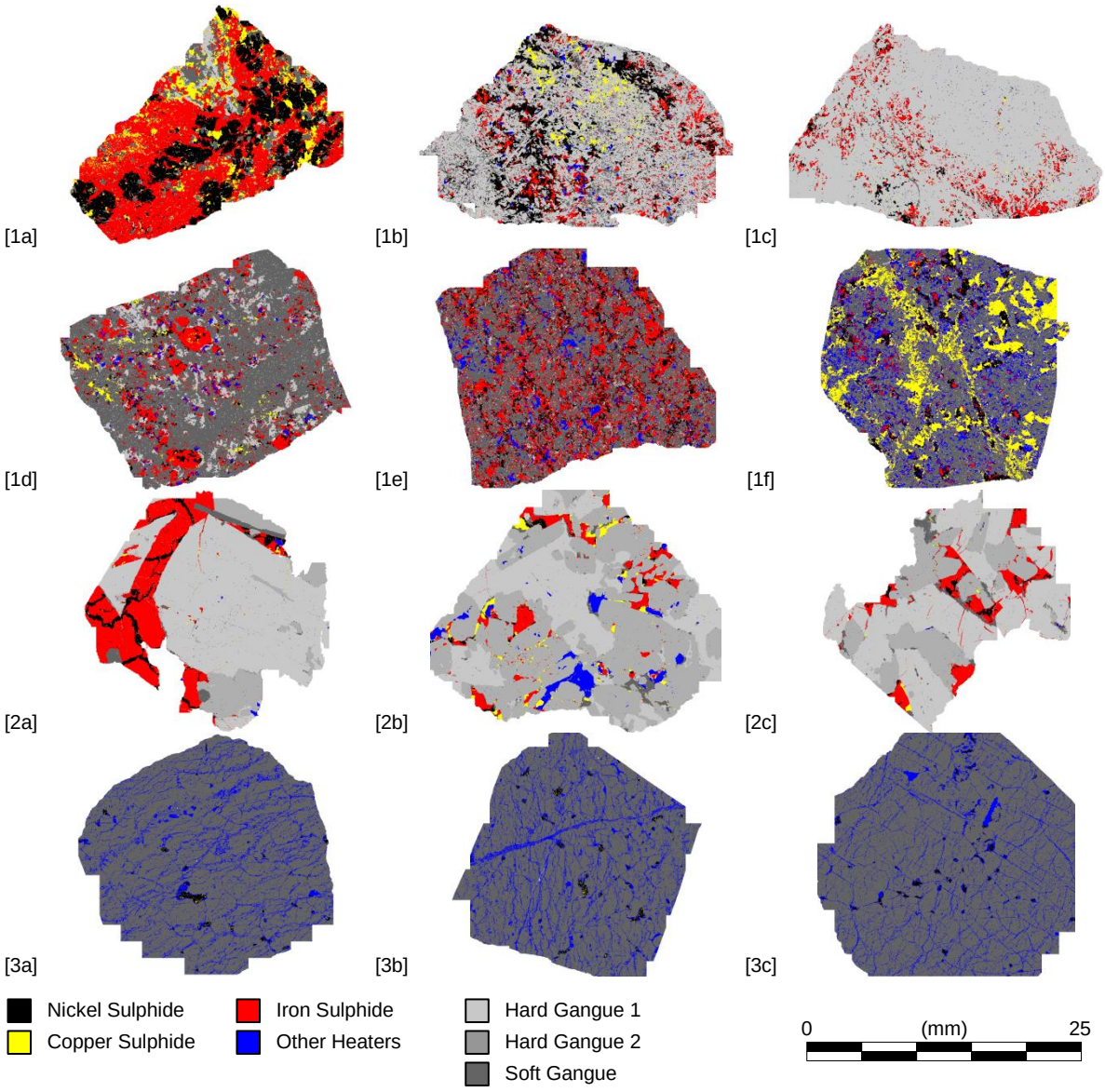

Figure 4: Nickel ore example lump fragment false colour images from MLA mineralogical texture analysis

http://dx.doi.org/10.1016/j.mineng.2015.10.007

3.1.2 Copper ores

Example MLA texture images for the five copper ores under investigation are given in Figure 5 with grouped mineral classifications of interest. The corresponding average modal mineralogy is given in Table 3.

Cu-Ore 1 and 2 were from the same porphyry copper host mine and were comprised of altered quartz monzonite characterised by the formation of illite, pyrophyllite and secondary sulphides. The two ores were very similar mineralogically but had a slightly different variety of textures. Cu-Ore 1 contained coarse sulphide to sulphide-barren fragments with both discrete and veined sulphide mineralisation. Another prevalent texture was other microwave-heating minerals (hydrated clays and iron oxides) associated with a soft gangue matrix. Cu-Ore 2 contained massive sulphide to sulphide-barren fragments with both discrete and veined sulphide mineralisation. For both ores, the sulphide minerals were typically associated with both a hard quartz and soft illite/pyrophyllite in the matrix.

Cu-Ore 3 and 4 were also both from the same porphyry copper host mine and both had consistent and yet differing textures. Cu-Ore 3 was a quartz monzonite ore that had sulphides and hydrated clays discretely disseminated throughout a speckled matrix comprised of hard quartz and feldspar, and soft biotite. Cu-Ore 4 was a quartzite ore that had sulphides and fine grained soft micas discretely mineralised and spread throughout a predominantly hard quartz matrix.

Cu-Ore 5 was a porphyry copper quartz monzonite breccia that had a fairly consistent speckled texture with discretely disseminated sulphides associated with hard quartz and feldspar, and soft muscovite in the matrix. Another common texture was rich in iron oxides and veined coarse grained sulphides.

Cu-Ore 6 was a porphyry copper dioritic breccia that had a consistent texture with discretely disseminated copper sulphides associated with a predominatly hard feldspar and quartz matrix.

Table 3: Modal mineralogy for the copper ores

Heating Class	Mineral Name	Modal Abundance (%wt)					
		Cu-Ore 1	Cu-Ore 2	Cu-Ore 3	Cu-Ore 4	Cu-Ore 5	Cu-Ore 6
Good-MW Heater	Chalcocite	1.2	1.5	0.0	<0.1	0.2	<0.1
	Chalcopyrite	0.6	1.2	0.9	1.1	1.4	0.8
	Covellite	0.2	0.3	0.0	0.0	0.1	0.1
	Bornite	0.5	0.8	0.0	0.1	0.2	0.0
	Pyrite [a]	5.7	9.8	1.8	1.1	1.2	0.1
	Smectite [b]	1.9	0.5	3.6	0.0	0.0	0.6
Poor-MW Heater	Iron Oxides [c]	1.3	0.3	0.3	<0.1	3.4	1.1
Non-MW Heating Gangue	Quartz	34.6	39.5	26.9	85.8	32.4	23.2
	Feldspar	4.0	1.8	39.8	0.1	28.7	71.4
	Mica-Phyllosilicate [d]	48.9	43.1	25.4	11.7	31.8	0.5
	Other	1.2	1.2	1.4	0.1	0.8	2.2

[a] Minor galena and molybdenite added to this group; [b] hydrous clays, typically classified as montmorillonite; [c] predominantly hematite with minor Fe/Ti oxides such as ilmenite and rutile added to this group; [d] predominantly illite for Cu-Ore 1 and 2, predominantly biotite for Cu-Ore 3 and 4, predominantly muscovite for Cu-Ore 5, predominantly chlorite for Cu-Ore 6, with typically minor amounts of illite, biotite, muscovite and chlorite plus kaolinite present in all the copper ores.

http://dx.doi.org/10.1016/j.mineng.2015.10.007

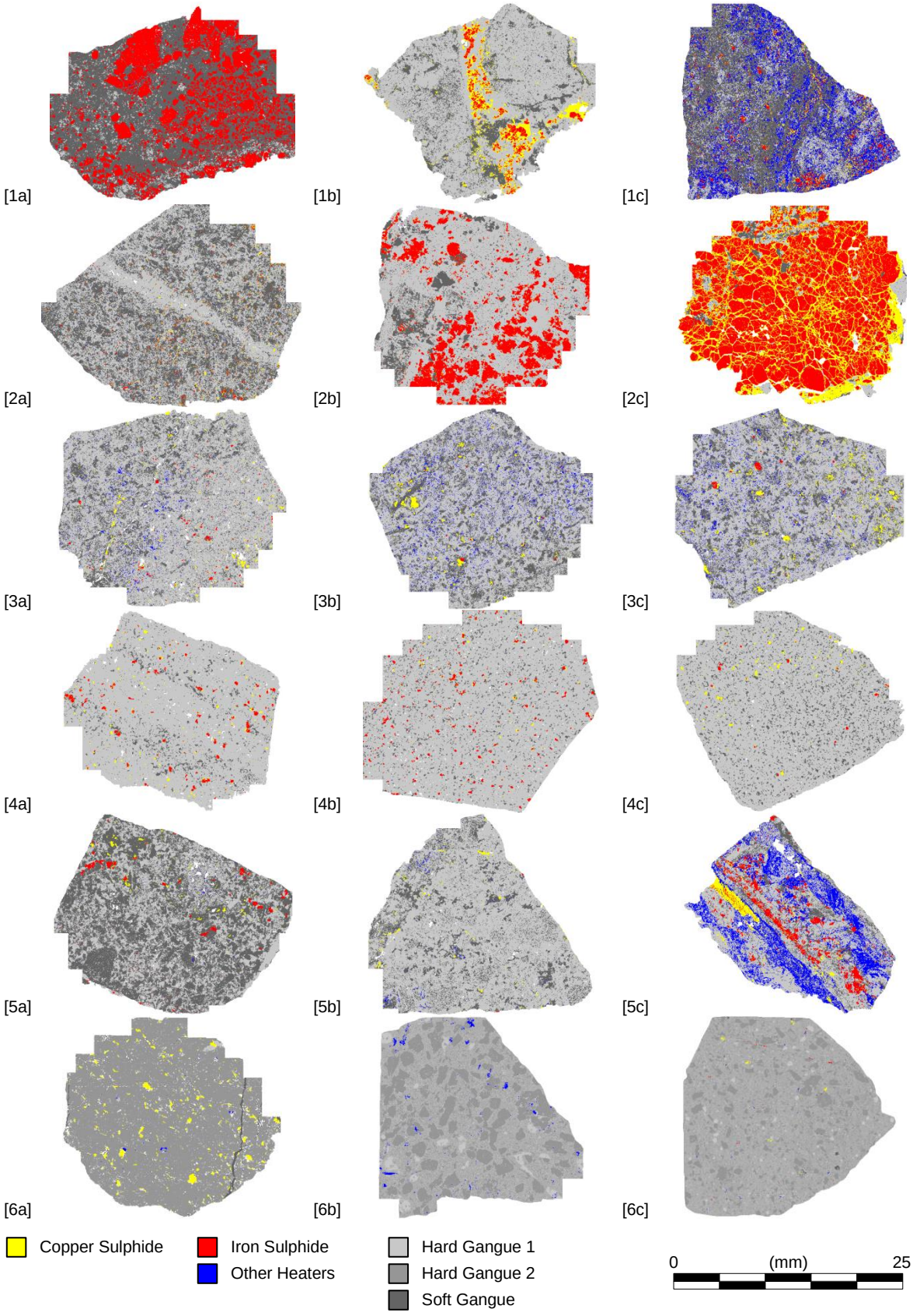

Figure 5: Copper ore example lump fragment false colour images from MLA mineralogical texture analysis

http://dx.doi.org/10.1016/j.mineng.2015.10.007

3.1.3 Lead-zinc ores

Example MLA texture images for the three of the four lead-zinc ores under investigation are given in Figure 6 with grouped mineral classifications of interest. The corresponding average modal mineralogy is given in Table 4.

Pb/Zn-Ore 1 and 2 were separate sedimentary rock hosted orebodies from the same host mine and both had consistent and yet differing textures. Pb/Zn-Ore 1 was a massive sulphide orebody with an abundance of coarse grained iron sulphides with more discretely disseminated sphalerite and magnetite highly associated with the iron sulphides in a soft illite and hard quartz speckled matrix. The Pb/Zn-Ore 2 orebody was frequently dominated by iron formation, effectively forming the matrix with associated hard quartz. Galena, sphalerite and iron sulphides were more discretely disseminated throughout the matrix while being highly associated with each other and magnetite.

Pb/Zn-Ore 3 was from a migmatitic quartzofeldspathic gneiss deposit with iron- and fluorite-rich gangue mineralisation. The ore had a fairly consistent texture with discretely disseminated coarse sulphides and magnetite predominantly associated with medium-hardness ferropyrosmalite and fluorite gangue despite an abundance of hard quartz and other silicates in the matrix.

Pb/Zn-Ore 4 was from a carbonate sedimentary rock hosted massive sulphide deposit but was not investigated using the MLA. However, a modal mineralogy of the test sample was provided by the host mine and upon visual inspection it appeared to have a similar texture to Pb/Zn-Ore 1 but with the non-sulphide gangue predominantly comprised of dolomite.

Table 4: Modal mineralogy for the lead-zinc ores

Heating Class	Mineral Name	Modal Abundance (%wt)			
		Pb/Zn-Ore 1	Pb/Zn-Ore 2	Pb/Zn-Ore 3	Pb/Zn-Ore 4
Good-MW Heater	Galena	0.6	4.9	13.4	0.5
	Chalcopyrite	0.1	0.6	0.2	-
	Iron Sulphides [a]	45.0	1.1	2.1	41.1
	Magnetite	4.0	73.0	10.5	-
Poor-MW Heater	Sphalerite	10.6	4.8	4.5	21.8
Non-MW Heating Gangue	Quartz	22.9	11.3	24.9	4.0
	Other Silicates [b]	1.6	2.2	17.1	2.0
	Mica-Phyllosilicate [c]	15.0	0.9	15.7	-
	Carbonates [d]	-	-	1.9	27.9
	Fluorite	-	-	9.9	-
	Other	0.3	1.2	0.3	2.7

[a] Predominantly pyrite with minor pyrrhotite and arsenopyrite; [b] roughly equal proportions of feldspar, garnet, amphibole, spinel, pyroxene and olivine; [c] predominantly illite in Pb/Zn-Ore 1 and predominantly ferropyrosmalite for Pb/Zn-Ore 3 with minor chlorite, biotite and talc in all three ores; [d] calcite for Pb/Zn-Ore 3 and predominantly dolomite for Pb/Zn-Ore 4 with some calcite.

http://dx.doi.org/10.1016/j.mineng.2015.10.007

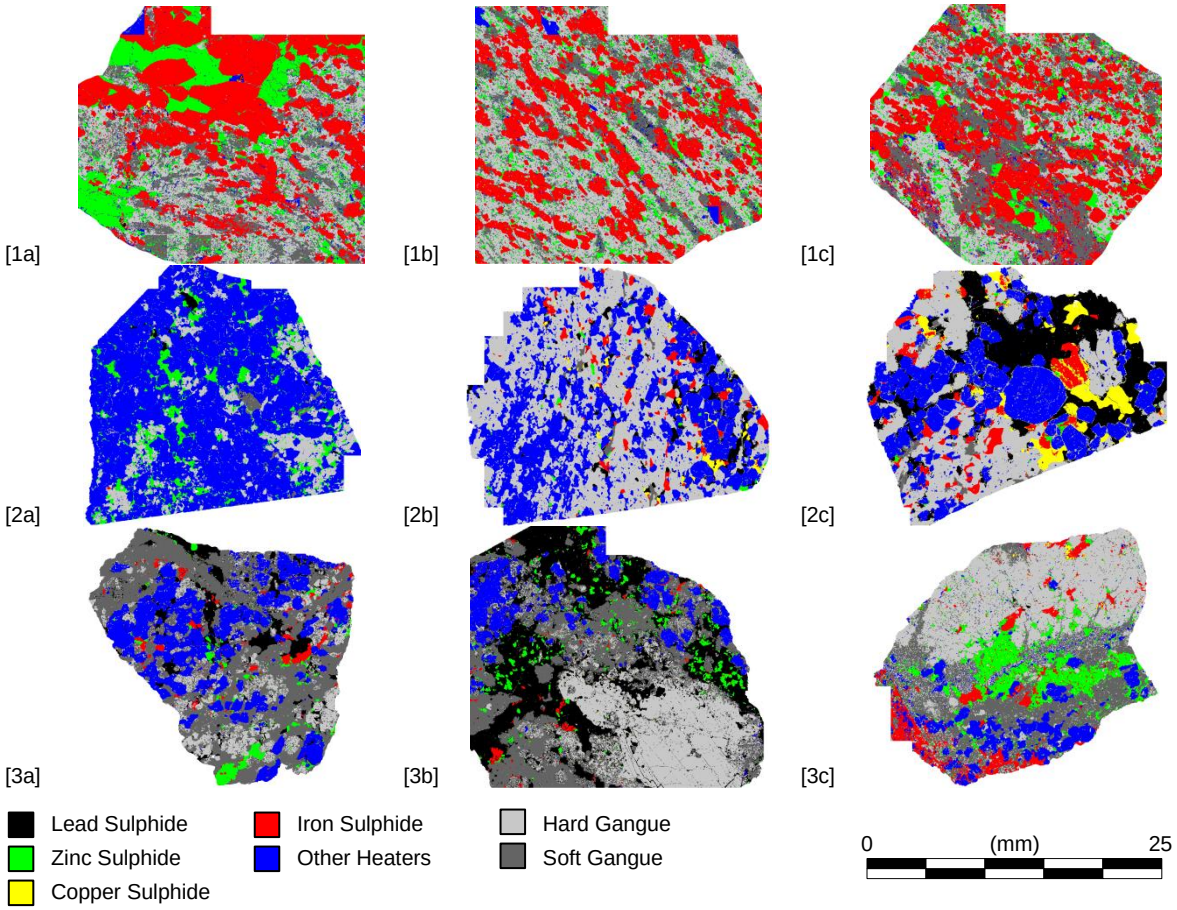

Figure 6: Lead-zinc ore example lump fragment false colour images from MLA mineralogical texture analysis

3.1.4 Summary

The good microwave-heating mineral phases in each ore were grouped and their grain size distributions extracted from the MLA texture evaluation, given in Figure 7. It must be noted that the measured apparent grain size distributions may appear artificially coarse due to the MLA software defining grain size as the diameter of an equivalent area circle. Many of the good microwave-heating phase grains occur as veins or otherwise touching adjacent grains. Any grains that touch are considered by the MLA software to be a single grain, thereby increasing the grain area and apparent grain size. Unfortunately, the MLA software offered no alternative option that would more representatively characterise the width and lengths of the adjoining grains to determine the average Feret's diameter.

The different ores demonstrated a wide range of good microwave-heating phase grain size distributions with which to consider the contribution of these minerals to microwave induced fracture in the ores. In order to summarise the grain size distributions into a single comparable value, the widest variation across the ores was chosen as the percent passing approximately 0.5mm to allow clear distinctions to be made between each ore. However, the variation of grain sizes across individual fragments must be considered for ores that have a variety of textures.

A comparison of the modal mineralogy of the ores grouped into classifications of interest is given in Figure 8. The chart shows a wide variety of sulphide and other heating phase abundance with the non-sulphide gangue divided into hard and soft minerals. The abundance of good microwave-heating phases ranged from approximately 2.5%wt to 60%wt and is predominantly comprised of iron sulphides for most ores under investigation. For three of the four lead-zinc ores, the non-valuable microwave-heating phases also comprised a significant proportion of the matrix. The abundance of hard gangue in the matrix ranges from approximately 0%wt to 86%wt and the abundance of soft gangue in the matrix ranges from approximately 1%wt to 50%wt. However, the variation of modal abundance and associations across individual fragments must also be considered for these ores, especially those with a variety of textures.

http://dx.doi.org/10.1016/j.mineng.2015.10.007

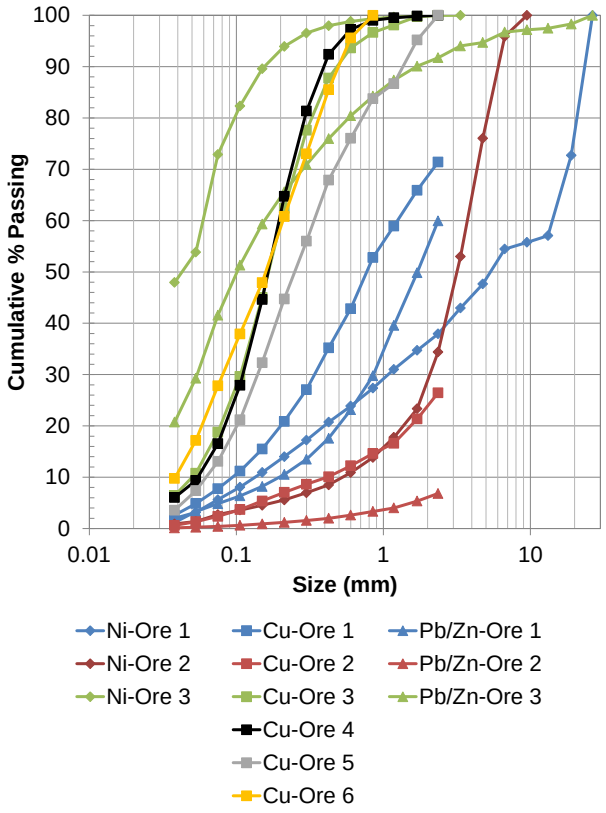

Figure 7: Apparent good microwave-heating phase grain size distributions

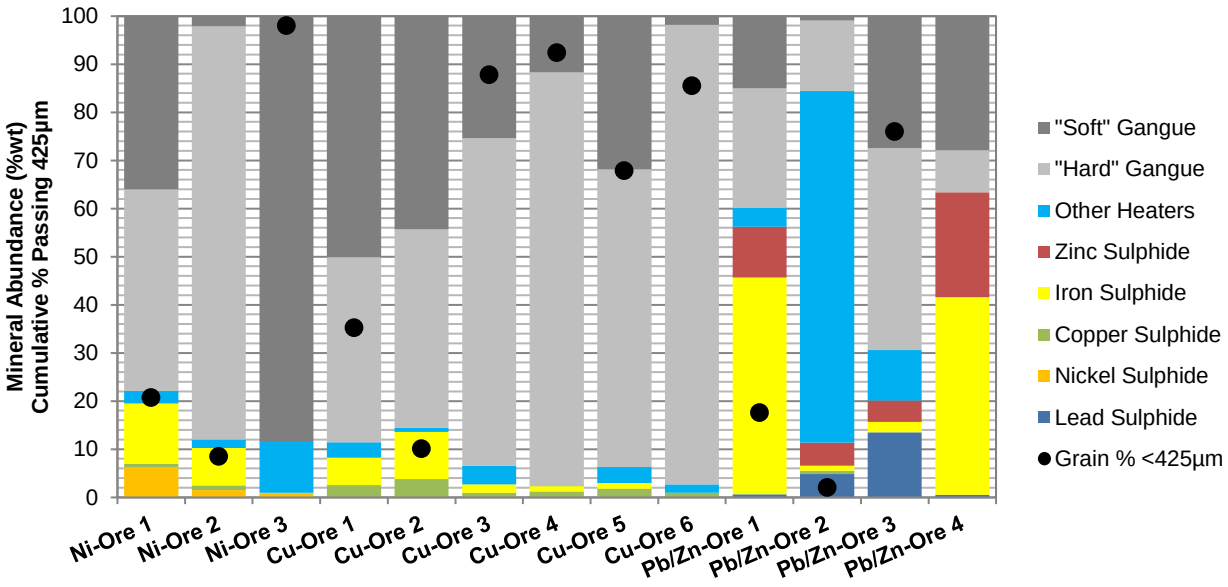

Figure 8: Modal mineralogy and good microwave-heating phase grain size comparison

http://dx.doi.org/10.1016/j.mineng.2015.10.007

3.2 Point Load Test results

Figure 9 to Figure 21 give the Point Load Index distributions for the 13 ores. As expected, each ore demonstrated a range of fragment strengths, reflecting the range of textures present in each ore. In other words, the ores that have a wider range of strengths tend to have many different textures present (e.g. Ni-Ore 1) and vice versa (e.g. Ni-Ore 3). However, even within similar textural groups there will be natural variation in fragment strength based on even slight variations in composition, association, grain size, natural flaws, etc.

The Point Load Index distributions for the microwave treated samples give an indication of the proportion of fragments that were affected by the microwave treatment. The proportion of affected fragments was also clearly dependent on the frequency of textures that were susceptible to microwave-induced fracture under the prevailing microwave treatment conditions. Many of the ores did not exhibit large changes in the Point Load Index distributions between untreated and treated ore, such as Ni-Ore 1, Cu-Ore 1, Cu-Ore 2, Cu-Ore 3, Cu-Ore 4, Cu-Ore 6 and Pb/Zn-Ore 4. This was due to a high proportion of unfavourable textures, such as the absence of good heaters, the microwave-heating phases being too finely disseminated or being constrained by a soft matrix.

In contrast, some ores demonstrated significant changes even at relatively low microwave energy inputs due to a high prevalence of favourable textures, such as Pb/Zn-Ore 2 and Pb/Zn-Ore 3 that contained coarse grained magnetite, which is an excellent microwave-heating mineral. A Point Load Index of zero was returned when either a fragment was broken during microwave treatment or was subsequently weakened to such an extent that the lowest measurable force from the Point Load tester did not register before breakage. Such fragments tended to break along planes or regions of coarse iron sulphide mineralisation, particularly for the nickel and copper ores tested.

It can be clearly seen how increasing the microwave energy can both increase the proportion of affected fragments and the severity of the microwave-induced fracturing by providing more energy to initiate and propagate fractures, such as with Ni-Ore 2, Ni-Ore 3 and Cu-Ore 3. For Ni-Ore 3 in particular, despite having a high proportion of magnetite, it was present as very fine grains constrained by a soft serpentine matrix, which required a greater amount of microwave energy to drive fracture propagation. Conversely, some ores did not exhibit significant changes in Point Load Index distribution with increasing microwave energy, such as Ni-Ore 1, Cu-Ore 5, Pb/Zn-Ore 1, Pb/Zn-Ore 2 and Pb/Zn-Ore 4. This was due to presence of some textures that fracture relatively easily at lower microwave energy inputs combined with other textures that required significantly higher microwave energy or power density than that used in these investigations, or due to realising all potential microwave-induced fracturing.

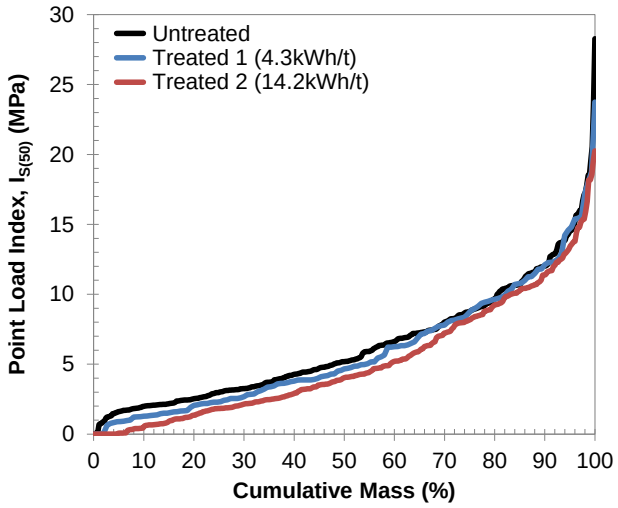

Figure 9: Point Load Test results for Ni-Ore 1

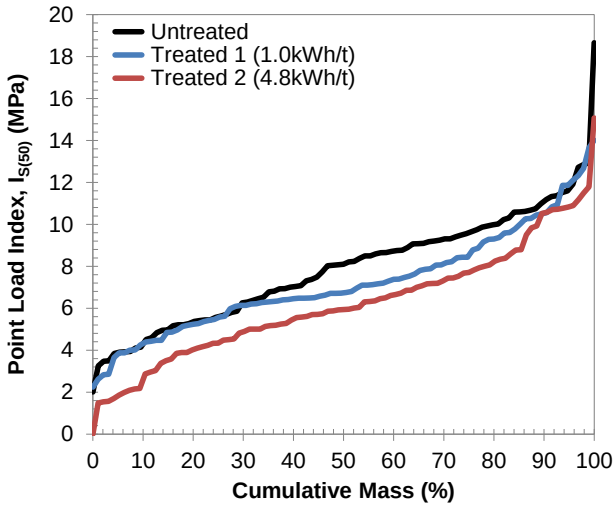

Figure 10: Point Load Test results for Ni-Ore 2

http://dx.doi.org/10.1016/j.mineng.2015.10.007

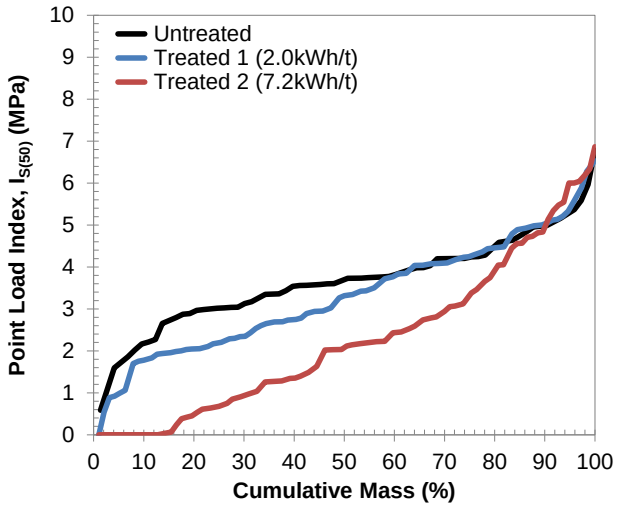

Figure 11: Point Load Test results for Ni-Ore 3

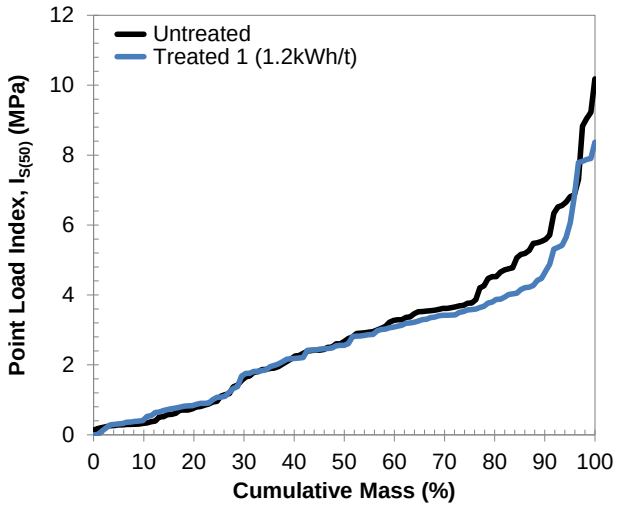

Figure 12: Point Load Test results for Cu-Ore 1

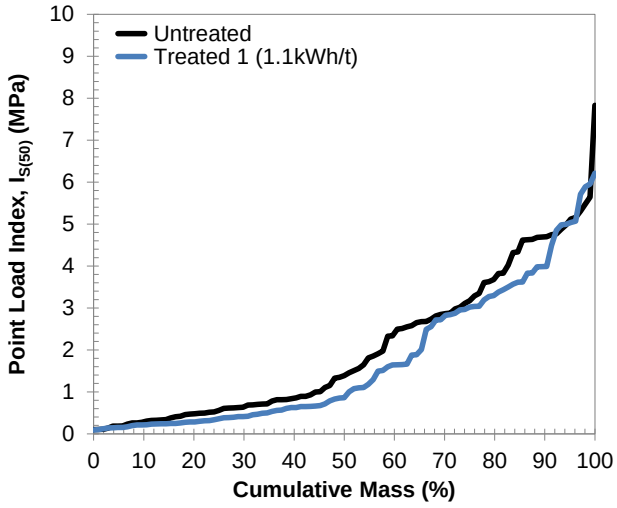

Figure 13: Point Load Test results for Cu-Ore 2

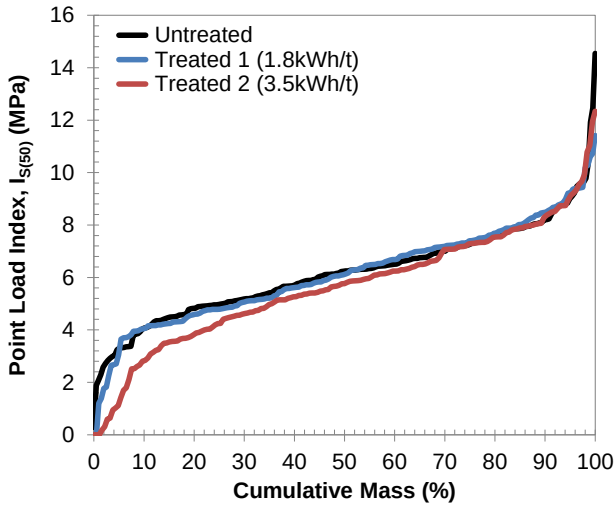

Figure 14: Point Load Test results for Cu-Ore 3

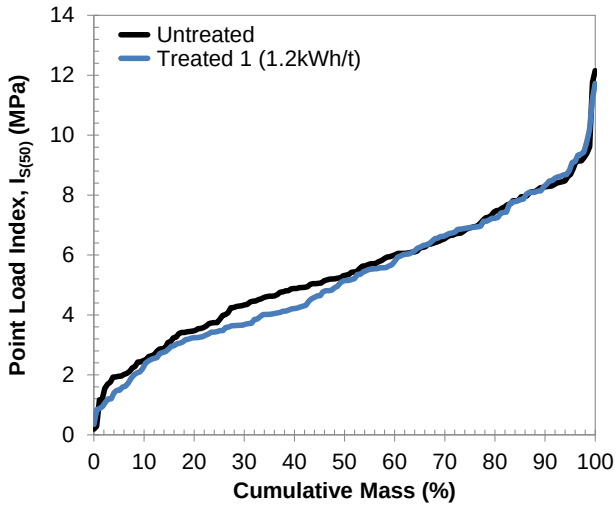

Figure 15: Point Load Test results for Cu-Ore 4

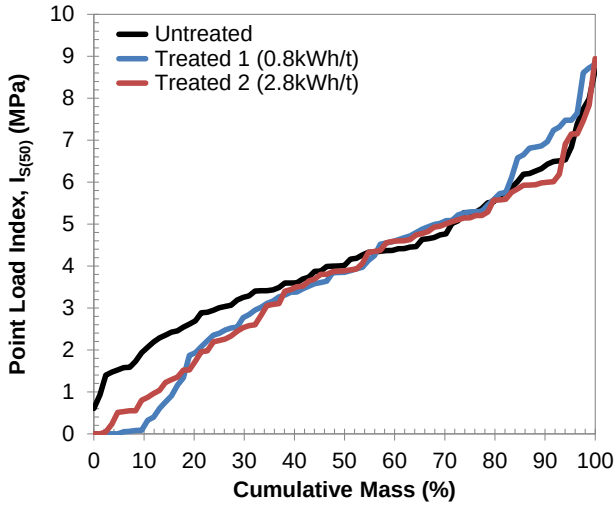

Figure 16: Point Load Test results for Cu-Ore 5

http://dx.doi.org/10.1016/j.mineng.2015.10.007

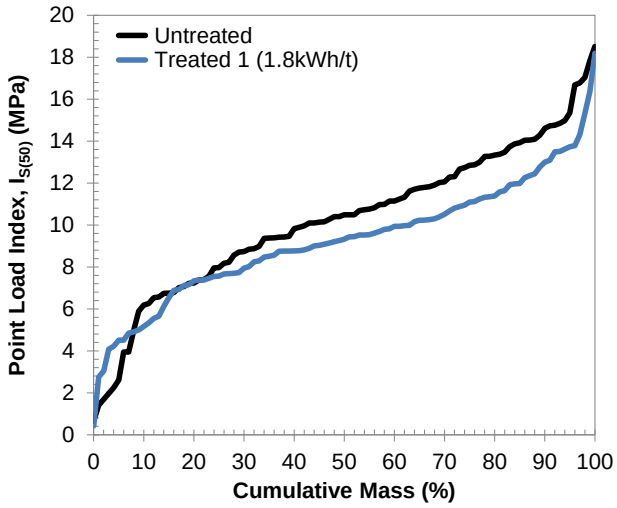

Figure 17: Point Load Test results for Cu-Ore 6

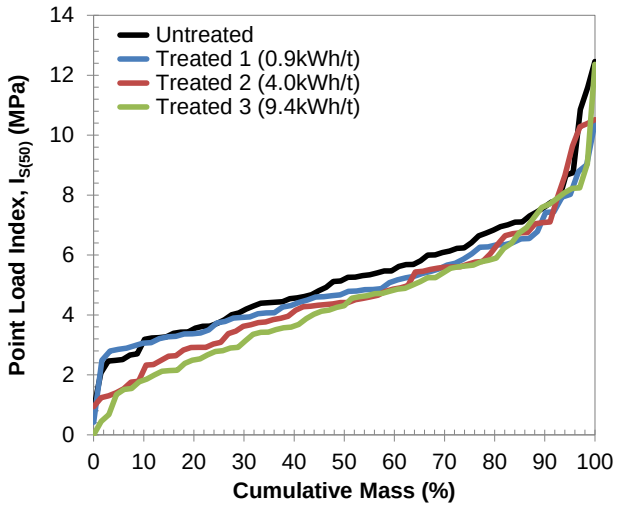

Figure 18: Point Load Test results for Pb/Zn-Ore 1

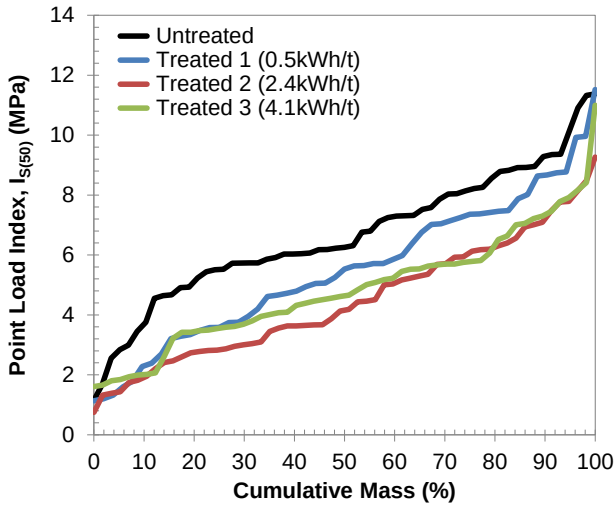

Figure 19: Point Load Test results for Pb/Zn-Ore 2

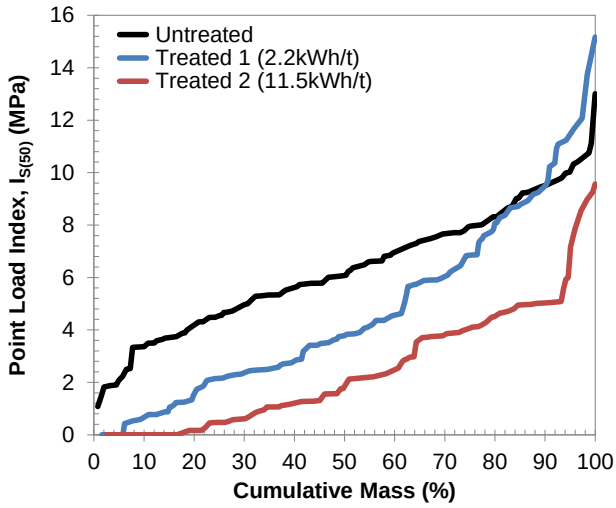

Figure 20: Point Load Test results for Pb/Zn-Ore 3

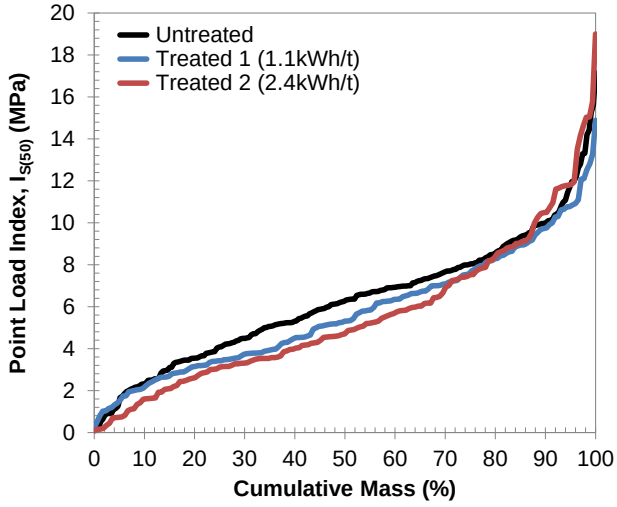

Figure 21: Point Load Test results for Pb/Zn-Ore 4

http://dx.doi.org/10.1016/j.mineng.2015.10.007

4 Discussion

Table 5 gives the average (mass weighted mean) Point Load Index results. Figure 22 shows the corresponding reductions in average Point Load Index after microwave treatment plotted as the percentage of the original strength remaining.

The ores that demonstrated the highest average reduction in Point Load Index (>20%) at lower microwave energies (less than ~5kWh/t) all contained a significant proportion of magnetite (Ni-Ore 3, Pb/Zn-Ore 2 and Pb/Zn-Ore 3). However, coarse grained magnetite coupled with a partially hard matrix was required to achieve high reductions at very low energies (less than ~1-2kWh/t) (Pb/Zn-Ore 2 and Pb/Zn-Ore 3).

The next best performing ores (>10% reduction at less than ~5kWh/t) typically contained a significant proportion of coarse iron sulphide mineralisation (Ni-Ore 2, Cu-Ore 2, Pb/Zn-Ore 1 and Pb/Zn-Ore 4). However, the better performing of these ores also tended to have a higher association with hard matrix minerals. The ores that did not achieve greater than 10% reduction tended to have a consistently fine good microwave-heating phase grain size, a high association with soft matrix minerals and/or a large proportion of barren fragments (Ni-Ore 1, Cu-Ore 1, Cu-Ore 3, Cu-Ore 4, Cu-Ore 5 and Cu-Ore 6).

Table 5: Average Point Load Index results

Sample ID	Mean Point Load Index, $I_{S(50)}$ (MPa)			
	Untreated	Treated 1	Treated 2	Treated 3
Ni-Ore 1	6.3	5.9	5.2	-
Ni-Ore 2	7.9	7.2	6.2	-
Ni-Ore 3	3.7	3.3	2.3	-
Cu-Ore 1	2.9	2.7	-	-
Cu-Ore 2	2.0	1.7	-	-
Cu-Ore 3	6.2	6.1	5.7	-
Cu-Ore 4	5.4	5.2	-	-
Cu-Ore 5	4.1	3.9	3.8	-
Cu-Ore 6	10.2	9.3	-	-
Pb/Zn-Ore 1	5.3	4.9	4.7	4.5
Pb/Zn-Ore 2	6.6	5.5	4.5	4.8
Pb/Zn-Ore 3	6.3	4.7	2.5	-
Pb/Zn-Ore 4	6.3	5.7	5.5	-

http://dx.doi.org/10.1016/j.mineng.2015.10.007

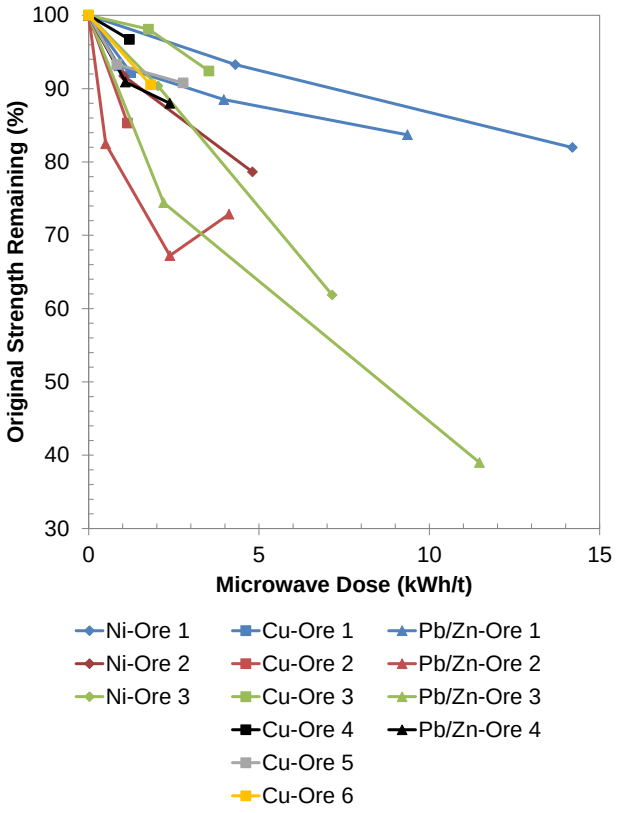

Figure 22: Point Load Test result summary

In general, these experimental results validate the theoretical models even though natural ores are highly heterogeneous by comparison. The most successful ores with respect to the highest average reduction in Point Load Index at the lowest microwave energy inputs typically met the following criteria:

- The presence of highly microwave-heating mineral phases, for example magnetite and lead, nickel, copper and iron sulphides.
- Approximately 2-20%wt total good microwave-heating phase abundance. For ores with greater than approximately 20%wt microwave-heating phases on average (e.g. massive sulphide deposits such as Pb/Zn-Ore 1 and Pb/Zn-Ore 4) or ores containing the majority of the good microwave-heating phases in lump sulphide fragments (e.g. Ni-Ore 1 and Cu-Ore 2), the microwave energy available to thermally expand the grains is reduced as it must be shared amongst the microwave-heating phases present. As such, significantly increasing the microwave treatment energy did not yield a corresponding significant reduction in strength for these ores. Therefore, microwave treatment may be unlikely to achieve large strength reductions on massive sulphide deposits at lower (more economically feasible) energy inputs unless other favourable properties are present.
- Approximately 50% of the matrix that constrains the microwave-heating minerals being comprised of hard minerals. A soft matrix may elastically absorb the thermal expansion, requiring higher microwave energy or power density to initiate and propagate fracture.
- A total microwave-heating phase grain size distribution with greater than approximately 50% of the grains coarser than 0.5mm.
- Well disseminated or veined microwave-heating phases within individual fragments. Such textures ensure that microwave-induced fracture occurs throughout the matrix of the fragment, rather than near the surface or edges of the fragment, thereby reducing the fragment competency.
- Texturally consistent with a high proportion of amenable textures. Such consistency ensures that the majority of the ore is affected by microwave treatment and large average reductions in ore strength can be realised.

http://dx.doi.org/10.1016/j.mineng.2015.10.007

Although large average strength reductions and subsequent changes in comminution energy requirements would not be expected in ores where there are a high proportion of barren fragments, favourable textures within the ore may still be amenable to microwave treatments. Considering the favourable textures within these ores would likely contain the majority of the valuable minerals of interest, other potential benefits of microwave treatment, such as improved liberation, might still be achieved. The potential for enhanced liberation and subsequent flotation should therefore be the focus of further investigations for these types of ores to determine if microwave treatment can add value to the operation other than direct reductions in comminution energy requirements.

5 Conclusions

The change in strength of a variety of ores that have undergone microwave treatment have been related to their mineralogical characteristics and treatment conditions, and compared against theoretical models in the literature. By validating simplistic two-phase model predictions with heterogeneous real ores it was possible to semi-quantitatively determine the ideal ore texture for microwave treatment with respect to reductions in ore competency as measured by the Point Load Index test.

The identified ranges of modal abundance, grain size distributions, thermo-mechanical properties and associations of microwave-absorbent phases with microwave-transparent phases in conjunction with qualitative assessments of dissemination throughout individual fragments and textural consistency across the ore samples have provided a baseline of least desirable to most desirable features for effective microwave treatment, given in Table 6. Given the limited number of ores investigated in this study no attempt has been made to prioritise the importance of different mineralogical and textural features. Therefore, this baseline is not intended to be prescriptive but to provide an opportunity to identify likely candidates for microwave treatment of ores in the future.

Table 6: Ideal ore properties matrix

Category			
Least Desirable	→ → → → → → →	→ → → → → → →	Most Desirable
Microwave-Heating Phase Heating Ability Occurences			
Non-Heater	Poor Heater	Good Heater	Excellent Heater
Good Microwave-Heating Phase Abundance			
<2%wt	>40%wt	20-40%wt	2-20%wt
Proportion of the Matrix Classified as ‘Hard’ (≥6 Mohs)			
<25%	25-50%	50-75%	>75%
Good Microwave-Heating Phase Grain Size (% >0.5mm)			
<15%	>90%	15-50%	50-90%
Good Microwave-Heating Phase Dissemination Occurences			
Heater Barren	Lump &/or Massive Heater	Clustered &/or Poorly Distributed	Veined &/or Well Distributed
Textural Consistency (Frequency of Amenable Textures)			
Few Amenable Textures	Some Amenable Textures	Several Amenable Textures	Many Amenable Textures

Acknowledgements

The authors would like to thank the sponsors of the AMIRA P879 and P879a projects for funding, supply of the ore materials and engagement throughout the projects.

http://dx.doi.org/10.1016/j.mineng.2015.10.007

References

Ali, A.Y., Bradshaw, S.M., 2009. Quantifying damage around grain boundaries in microwave treated ores. Chemical Engineering and Processing: Process Intensification 48, 1566-1573.

Ali, A.Y., Bradshaw, S.M., 2010. Bonded-particle modelling of microwave-induced damage in ore particles. Minerals Engineering 23, 780-790.

Ali, A.Y., Bradshaw, S.M., 2011. Confined particle bed breakage of microwave treated and untreated ores. Minerals Engineering 24, 1625-1630.

Batchelor, A.R., 2013. Microwave treatment of ores, Department of Chemical and Environmental Engineering. The University of Nottingham, Nottingham, UK.

Batterham, R., 2011. Trends in comminution driven by energy. Advanced Powder Technology 22, 138-140.

BCS, 2007. Mining industry energy bandwidth study. U.S. Department of Energy.

Broch, E., Franklin, J.A., 1972. The point-load strength test. International Journal of Rock Mechanics and Mining Sciences & Geomechanics Abstracts 9, 669-676.

Brook, N., 1985. The equivalent core diameter method of size and shape correction in point load testing. International Journal of Rock Mechanics and Mining Sciences & Geomechanics Abstracts 22, 61-70.

Chen, T., Dutrizac, J., Haque, K., Wyslouzil, W., Kashyap, S., 1984. The relative transparency of minerals to microwave radiation. Canadian Metallurgical Quarterly 23, 349-351.

Chunpeng, L., Yousheng, X., Yixin, H., 1990. Application of microwave radiation to extractive metallurgy. Journal of Materials Science and Technology (China) 6, 121-124.

Church, R.H., Webb, W.E., Salsman, J., 1988. Dielectric properties of low-loss minerals. US Department of the Interior, Volume 9194 of Report of Investigations, US Bureau of Mines.

Cooke, D.R., Hollings, P., Walshe, J.L., 2006. Giant porphyry deposits: characteristics, distribution, and tectonic controls. Economic Geology 100, 801-818.

Crowson, P., 2012. Some observations on copper yields and ore grades. Resources Policy 37, 59-72.

Curry, J.A., Ismay, M.J.L., Jameson, G.J., 2014. Mine operating costs and the potential impacts of energy and grinding. Minerals Engineering 56, 70-80.

Daniel, M., Lewis-Gray, E., 2011. Comminution efficiency attracts attention. The AusIMM Bulletin 5, 18-28.

Drinkwater, D., Napier-Munn, T.J., Ballantyne, G., 2012. Energy reduction through eco-efficient comminution strategies, 26th International Mineral Processing Congress, IMPC 2012: Innovative Processing for Sustainable Growth-Conference Proceedings. Technowrites, pp. 1223-1229.

Fitzgibbon, K.E., Veasey, T.J., 1990. Thermally assisted liberation - a review. Minerals Engineering 3, 181-185.

Franklin, J.A., 1985. Suggested method for determining point load strength. International Journal of Rock Mechanics and Mining Sciences & Geomechanics Abstracts 22, 51-60.

Haque, K.E., 1999. Microwave energy for mineral treatment processes—a brief review. International Journal of Mineral Processing 57, 1-24.

Harrison, P.C., 1997. A fundamental study of the effects of 2.45GHz microwave radiation on the properties of minerals. The University of Birmingham, Birmingham, UK.

Jones, D.A., Kingman, S.W., Whittles, D.N., Lowndes, I.S., 2005. Understanding microwave assisted breakage. Minerals Engineering 18, 659-669.

Jones, D.A., Kingman, S.W., Whittles, D.N., Lowndes, I.S., 2007. The influence of microwave energy delivery method on strength reduction in ore samples. Chemical Engineering and Processing: Process Intensification 46, 291-299.

Jones, D.A., Lelyveld, T.P., Mavrofidis, S.D., Kingman, S.W., Miles, N.J., 2002. Microwave heating applications in environmental engineering—a review. Resources, Conservation and Recycling 34, 75-90.

http://dx.doi.org/10.1016/j.mineng.2015.10.007

Kesler, S.E., 2007. Mineral supply and demand into the 21st century, US Geological Survey circular 1294: proceedings for a workshop on deposit modeling, mineral resource assessment, and their role in sustainable development. Reston, VA: US Geological Survey, pp. 55-62.

Kingman, S.W., Jackson, K., Bradshaw, S.M., Rowson, N.A., Greenwood, R., 2004a. An investigation into the influence of microwave treatment on mineral ore comminution. Powder Technology 146, 176-184.

Kingman, S.W., Jackson, K., Cumbane, A., Bradshaw, S.M., Rowson, N.A., Greenwood, R., 2004b. Recent developments in microwave-assisted comminution. International Journal of Mineral Processing 74, 71-83.

Kingman, S.W., Rowson, N.A., 1998. Microwave treatment of minerals-a review. Minerals Engineering 11, 1081-1087.

Kingman, S.W., Vorster, W., Rowson, N.A., 2000a. The effect of microwave radiation on the processing of Palabora copper ore. Journal of the South African Institute of Mining and Metallurgy 100, 197-204.

Kingman, S.W., Vorster, W., Rowson, N.A., 2000b. The influence of mineralogy on microwave assisted grinding. Minerals Engineering 13, 313-327.

Kobusheshe, J., 2010. Microwave enhanced processing of ores. University of Nottingham, Nottingham, UK.

McGill, S., Walkiewicz, J., 1987. Applications of microwave energy in extractive metallurgy. Journal of Microwave Power and Electromagnetic Energy 22, 175-177.

McGill, S., Walkiewicz, J., Smyres, G., 1988. The effects of power level on the microwave heating of selected chemicals and minerals, Materials Research Society Proceedings. Cambridge University Press, pp. 247-252.

Meredith, R.J., 1998. Engineers' handbook of industrial microwave processing. The Institution of Electrical Engineers, London, UK.

Mudd, G.M., 2010. The Environmental sustainability of mining in Australia: key mega-trends and looming constraints. Resources Policy 35, 98-115.

Mudd, G.M., Weng, Z., Jowitt, S.M., 2013. A detailed assessment of global Cu resource trends and endowments. Economic Geology 108, 1163-1183.

Nadolski, S., Klein, B., Kumar, A., Davaanyam, Z., 2014. An energy benchmarking model for mineral comminution. Minerals Engineering 65, 178-186.

Nelson, S., Lindroth, D., Blake, R., 1989. Dielectric properties of selected minerals at 1 to 22 GHz. Geophysics 54, 1344-1349.

Norgate, T., Jahanshahi, S., 2011. Reducing the greenhouse gas footprint of primary metal production: Where should the focus be? Minerals Engineering 24, 1563-1570.

Northey, S., Mohr, S., Mudd, G.M., Weng, Z., Giurco, D., 2014. Modelling future copper ore grade decline based on a detailed assessment of copper resources and mining. Resources, Conservation and Recycling 83, 190-201.

Pokrajcic, Z., Morrison, R., Johnson, B., 2009. Designing for a reduced carbon footprint at Greenfield and operating comminution plants, Recent Advances in Mineral Processing Plant Design. Society for Mining, Metallurgy, and Exploration, pp. 560-570.

Powell, M., Bye, A., 2009. Beyond mine-to-mill: Circuit design for energy efficient resource utilisation, Tenth Mill Operators Conference 2009, Proceedings. AusIMM, pp. 357-364.

Prior, T., Giurco, D., Mudd, G., Mason, L., Behrisch, J., 2012. Resource depletion, peak minerals and the implications for sustainable resource management. Global Environmental Change 22, 577-587.

Sahyoun, C., Rowson, N., Kingman, S., Groves, L., Bradshaw, S., 2005. The influence of microwave pre-treatment on copper flotation. Journal of the South African Institute of Mining and Metallurgy 105, 7-14.

Salsman, J.B., Williamson, R.L., Tolley, W.K., Rice, D.A., 1996. Short-pulse microwave treatment of disseminated sulfide ores. Minerals Engineering 9, 43-54.

Sillitoe, R.H., 2010. Porphyry copper systems. Economic Geology 105, 3-41.

Standish, N., Worner, H., 1991. Microwave application in the reduction of metal oxides with carbon. Iron & Steelmaker 18, 59-61.

Tromans, D., 2008. Mineral comminution: Energy efficiency considerations. Minerals Engineering 21, 613-620.

http://dx.doi.org/10.1016/j.mineng.2015.10.007

Veasey, T.J., Wills, B.A., 1991. Review of methods of improving mineral liberation. Minerals Engineering 4, 747-752.

Walkiewicz, J., Kazonich, G., McGill, S., 1988. Microwave heating characteristics of selected minerals and compounds. Minerals and Metallurgical Processing 5, 39-42.

Wang, G., Radziszewski, P., Ouellet, J., 2008. Particle modeling simulation of thermal effects on ore breakage. Computational Materials Science 43, 892-901.

Wang, Y., Djordjevic, N., 2014. Thermal stress FEM analysis of rock with microwave energy. International Journal of Mineral Processing 130, 74-81.

Whittles, D.N., Kingman, S.W., Reddish, D.J., 2003. Application of numerical modelling for prediction of the influence of power density on microwave-assisted breakage. International Journal of Mineral Processing 68, 71-91.

Yixin, H., Chunpeng, L., 1996. Heating rate of minerals and compounds in microwave field. Transactions of Non-Ferrous Metals Society of China 6, 35-40.

http://dx.doi.org/10.1016/j.mineng.2015.10.007